



A Lagrange multiplier method for flow in fractured poroelastic media

Eldar Khattatov[†], Ivan Yotov[†], Ilona Ambartsumyan[†], Paolo Zunino[‡]

[†] Department of Mathematics, University of Pittsburgh, Pittsburgh, Pennsylvania, USA;

[‡] Department of Mechanical Engineering & Materials Science, University of Pittsburgh, Pittsburgh, Pennsylvania, USA;

1. Model Problem: Coupled Stokes-Biot System

- Groundwater flow and flow in fractured porous media
- Cardiovascular flow

Figure 1. Applications

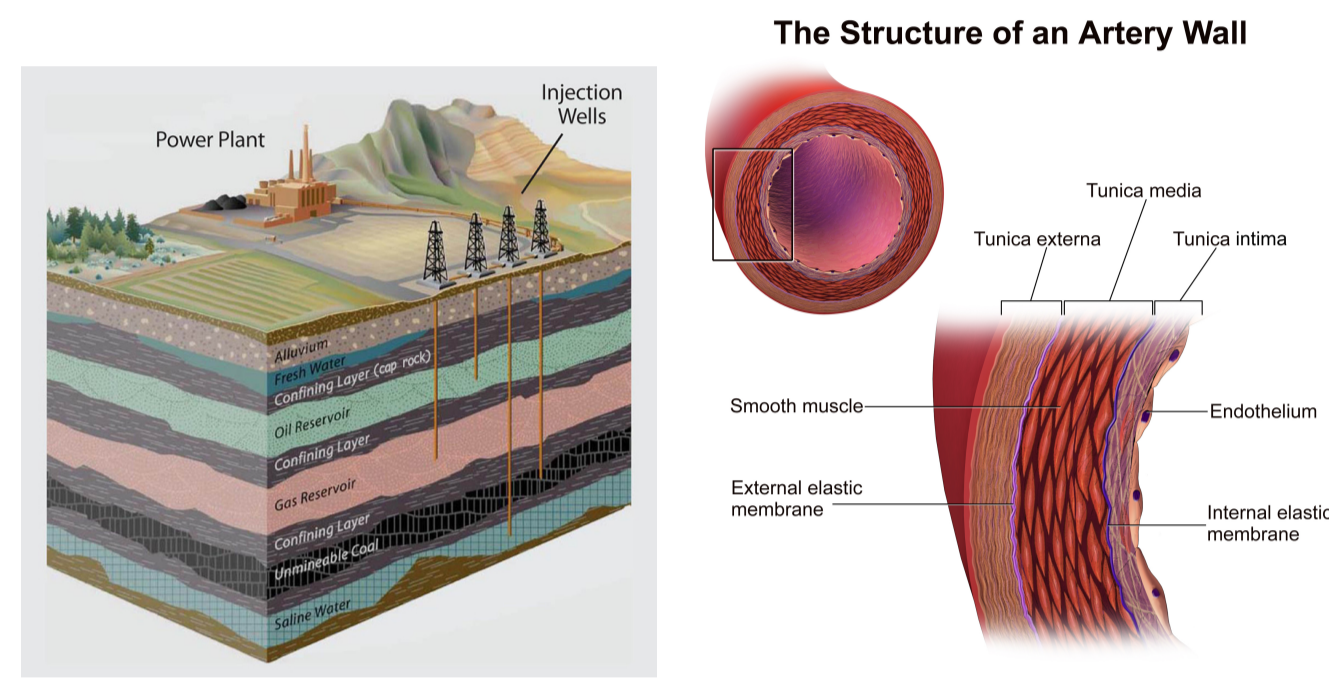
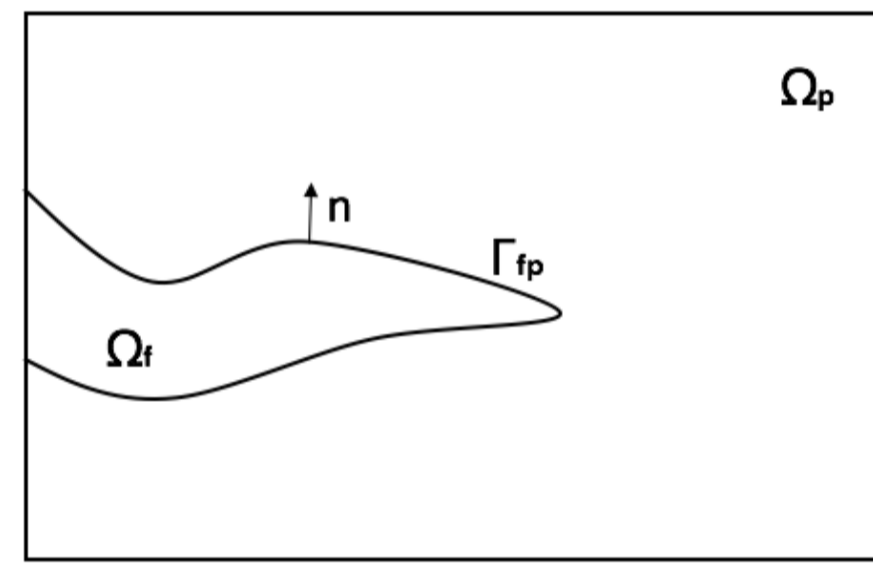


Figure 2. Stokes-Biot model



Biot system of poroelasticity in Ω_p :

\mathbf{u}_p = Darcy velocity, p_p = pressure, $\boldsymbol{\eta}$ = displacement

$$\begin{aligned} -\nabla \cdot \boldsymbol{\sigma}_p(\boldsymbol{\eta}) &= \mathbf{f}_p \\ \frac{\partial}{\partial t}(s_0 p_p + \alpha \nabla \cdot \boldsymbol{\eta}) + \nabla \cdot \mathbf{u}_p &= q_p, \\ \mathbf{K}^{-1} \mathbf{u}_p &= -\nabla p_p, \end{aligned}$$

where $\boldsymbol{\sigma}_p(\boldsymbol{\eta}) = \lambda_p(\nabla \cdot \boldsymbol{\eta})\mathbf{I} + 2\mu_p \mathbf{D}(\boldsymbol{\eta}) - \alpha p_p \mathbf{I}$ is a poroelastic stress tensor, α is Biot-Willis constant and \mathbf{K} is a permeability tensor.

Stokes flow in Ω_f :

\mathbf{u}_f = Stokes velocity, p_f = fluid pressure

$$\begin{aligned} \rho_f \frac{\partial \mathbf{u}_f}{\partial t} - \nabla \cdot \boldsymbol{\sigma}_f &= \mathbf{f}_f, \\ \nabla \cdot \mathbf{u}_f &= q_f, \end{aligned}$$

where $\boldsymbol{\sigma}_f = -p_f \mathbf{I} + 2\mu_f \mathbf{D}(\mathbf{u}_f)$ is a Cauchy stress tensor.

Interface conditions on Γ_{fp} :

Mass conservation:

$$\mathbf{u}_f \cdot \mathbf{n} = \left(\frac{\partial \boldsymbol{\eta}}{\partial t} + \mathbf{u}_p \right) \cdot \mathbf{n}$$

Balance of normal fluid stress:

$$-(\boldsymbol{\sigma}_f \mathbf{n}) \cdot \mathbf{n} = p_p$$

Continuity of momentum:

$$\boldsymbol{\sigma}_f \mathbf{n} = \boldsymbol{\sigma}_p \mathbf{n}$$

No slip or Beavers-Joseph-Saffman condition:

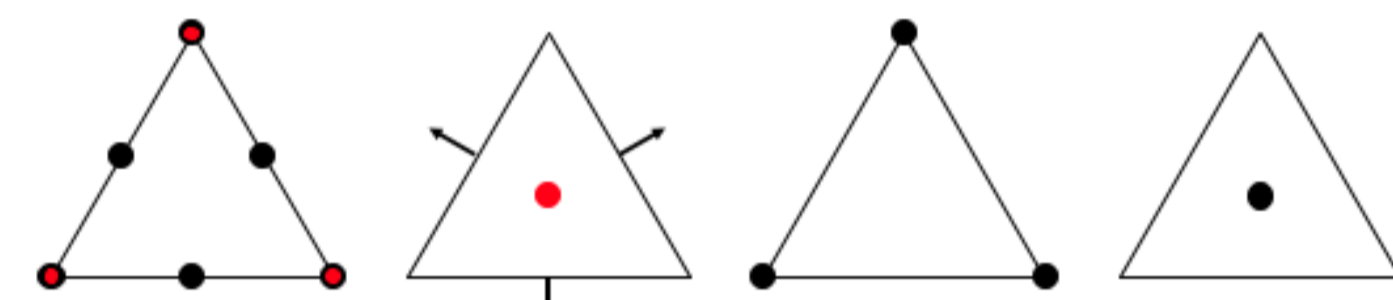
- $\mathbf{u}_f \cdot \boldsymbol{\tau} = \frac{\partial \boldsymbol{\eta}}{\partial t} \cdot \boldsymbol{\tau}$
- $-(\boldsymbol{\sigma}_f \mathbf{n}) \cdot \boldsymbol{\tau} = c_{BJS}(\mathbf{u}_f - \frac{\partial \boldsymbol{\eta}}{\partial t}) \cdot \boldsymbol{\tau}$

2. Discretization & numerical analysis

The discretization

- is derived on simplicial grids in 2D and 3D;
- uses standard conforming finite elements for Stokes and elasticity equations and mixed finite elements for Darcy;
- allows the fluid and poroelastic region grids to be non-matching through the interface;
- utilizes a Lagrange multiplier λ on the interface to weakly impose the continuity of flux;
- uses the space for λ being the normal trace of Darcy velocity space.

Figure 3. Example of lowest order FE spaces: $(\mathcal{P}_2 \times \mathcal{P}_1) \times (\mathcal{RT}_0 \times \mathcal{P}_0) \times \mathcal{P}_1 \times \mathcal{P}_0$



Discrete weak formulation

Find $(\mathbf{u}_{f,h}, p_{f,h}, \mathbf{u}_{p,h}, p_{p,h}, \boldsymbol{\eta}_{p,h}, \lambda_h)$ in $\mathbf{V}_{f,h} \times W_{f,h} \times \mathbf{V}_{p,h} \times W_{p,h} \times \mathbf{X}_{p,h} \times \Lambda_h$ such that

$$\begin{aligned} (\rho_f \partial_t \mathbf{u}_{f,h}, \mathbf{v}_{f,h}) + a_f(\mathbf{u}_{f,h}, \mathbf{v}_{f,h}) + a_p^d(\mathbf{u}_{p,h}, \mathbf{v}_{p,h}) + a_p^e(\boldsymbol{\eta}_{p,h}, \boldsymbol{\xi}_{p,h}) \\ + a_{BJS}(\mathbf{u}_{f,h}, \boldsymbol{\eta}_{p,h}; \mathbf{v}_{f,h}, \boldsymbol{\xi}_{p,h}) + b_f(\mathbf{v}_{f,h}, p_{f,h}) + b_p(\mathbf{v}_{p,h}, p_{p,h}) \\ + \alpha b_p(\boldsymbol{\xi}_{p,h}, p_{p,h}) + b_\Gamma(\mathbf{v}_{f,h}, \mathbf{v}_{p,h}; \boldsymbol{\xi}_{p,h}; \lambda_h) = \mathbf{f}(\mathbf{v}_{f,h}, \boldsymbol{\xi}_{p,h}), \\ (\partial_t s_0 p_{p,h}, w_{p,h}) - \alpha b_p(\partial_t \boldsymbol{\eta}_{p,h}, w_{p,h}) - b_p(\mathbf{u}_{p,h}, w_{p,h}) \\ - b_f(\mathbf{u}_{f,h}, w_{f,h}) = q(w_{f,h}, w_{p,h}), \\ b_\Gamma(\mathbf{u}_{f,h}, \mathbf{u}_{p,h}; \partial_t \boldsymbol{\eta}_{p,h}; \mu_h) = 0, \end{aligned}$$

With Backward Euler used for discrete time derivative

$$d_\tau u^n := \tau^{-1}(u^n - u^{n-1})$$

Convergence analysis of the discrete formulation

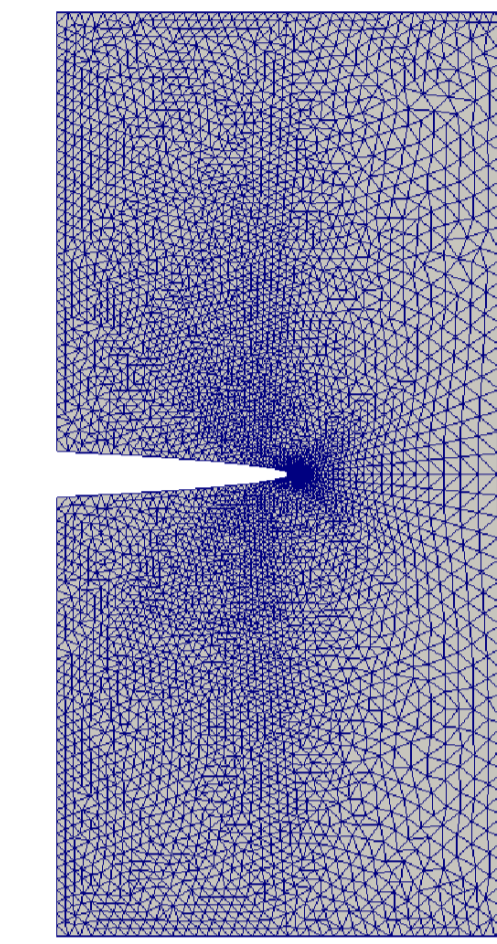
With k_f, s_f, k_p, s_p, k_s denoting the order of polynomials used in the discretization of Stokes, Darcy and elasticity equations respectively, there holds

$$\begin{aligned} \|\mathbf{u}_f - \mathbf{u}_{f,h}\|_{L^\infty(L^2)} + \|\mathbf{u}_f - \mathbf{u}_{f,h}\|_{L^2(H^1)} + \|\mathbf{u}_p - \mathbf{u}_{p,h}\|_{L^2(L^2)} \\ + \|p_p - p_{p,h}\|_{L^\infty(L^2)} + \|\boldsymbol{\eta}_p - \boldsymbol{\eta}_{p,h}\|_{L^\infty(H^1)} \\ + \sum_{j=1}^{d-1} \nu c_{BJS} \|\mathbf{K}_j^{-1/4} ((\mathbf{u}_f - \mathbf{u}_{f,h}) - \partial_t(\boldsymbol{\eta}_p - \boldsymbol{\eta}_{p,h})) \cdot \boldsymbol{\tau}_{f,j}\|_{L^2(L^2(\Gamma_{fp}))} \\ \leq C \left(h^{k_f} \|\mathbf{u}_f\|_{L^2(H^{k_f+1})} + h^{k_f} \|\mathbf{u}_f\|_{L^\infty(H^{k_f+1})} + h^{k_f} \|\partial_t \mathbf{u}_f\|_{L^2(H^{k_f+1})} \right. \\ \left. + h^{s_f+1} \|p_f\|_{L^2(H^{s_f+1})} + h^{k_p+1} \|\mathbf{u}_p\|_{L^2(H^{k_p+1})} + h^{k_s} \|\partial_t \boldsymbol{\eta}_p\|_{L^2(H^{k_s+1})} \right. \\ \left. + h^{k_p+1} \|\lambda\|_{L^2(H^{k_p+1}(\Gamma_{fp}))} + h^{k_s} \|\boldsymbol{\eta}_p\|_{L^\infty(H^{k_s+1})} + h^{k_p+1} \|\lambda\|_{L^\infty(H^{k_p+1}(\Gamma_{fp}))} \right. \\ \left. + h^{s_p+1} \|p_p\|_{L^\infty(H^{s_p+1})} + h^{k_p+1} \|\partial_t \lambda\|_{L^2(H^{k_p+1}(\Gamma_{fp}))} + h^{s_p+1} \|p_p\|_{L^2(H^{s_p+1})} \right) \end{aligned}$$

3. Convergence, BJS condition and continuity of flux

Convergence study on a reference domain

Figure 4. Reference grid



Parameter	Units	Value
Young's modulus	(Pa)	10^{10}
Fluid density	(kg/m ³)	1.0
Dynamic viscosity	(Pa s)	1.0
Lame coefficient	(Pa)	$5/12 \cdot 10^{10}$
Lame coefficient	(Pa)	$5/18 \cdot 10^{10}$
Hydraulic conductivity	(m ² /Pa s)	1d
Mass storativity	(Pa ⁻¹)	1.0
Biot-Willis constant		1.0
BJS coefficient		1.0
Total time	(s)	1.0

$$\begin{aligned} \mathbf{u}_f \cdot \mathbf{n} &= 10, \mathbf{u}_f \cdot \boldsymbol{\tau} = 0 \text{ on } \Gamma_{inflow} \\ \mathbf{u}_p \cdot \mathbf{n} &= 0, \text{ on } \Gamma_{left} \\ p_p &= 0, \text{ on } \Gamma_{top} \cup \Gamma_{right} \cup \Gamma_{bottom} \\ \boldsymbol{\eta} &= 0, \text{ on } \Gamma_{top} \cup \Gamma_{right} \cup \Gamma_{bottom} \end{aligned}$$

Table 1. Convergence study using the lowest order elements

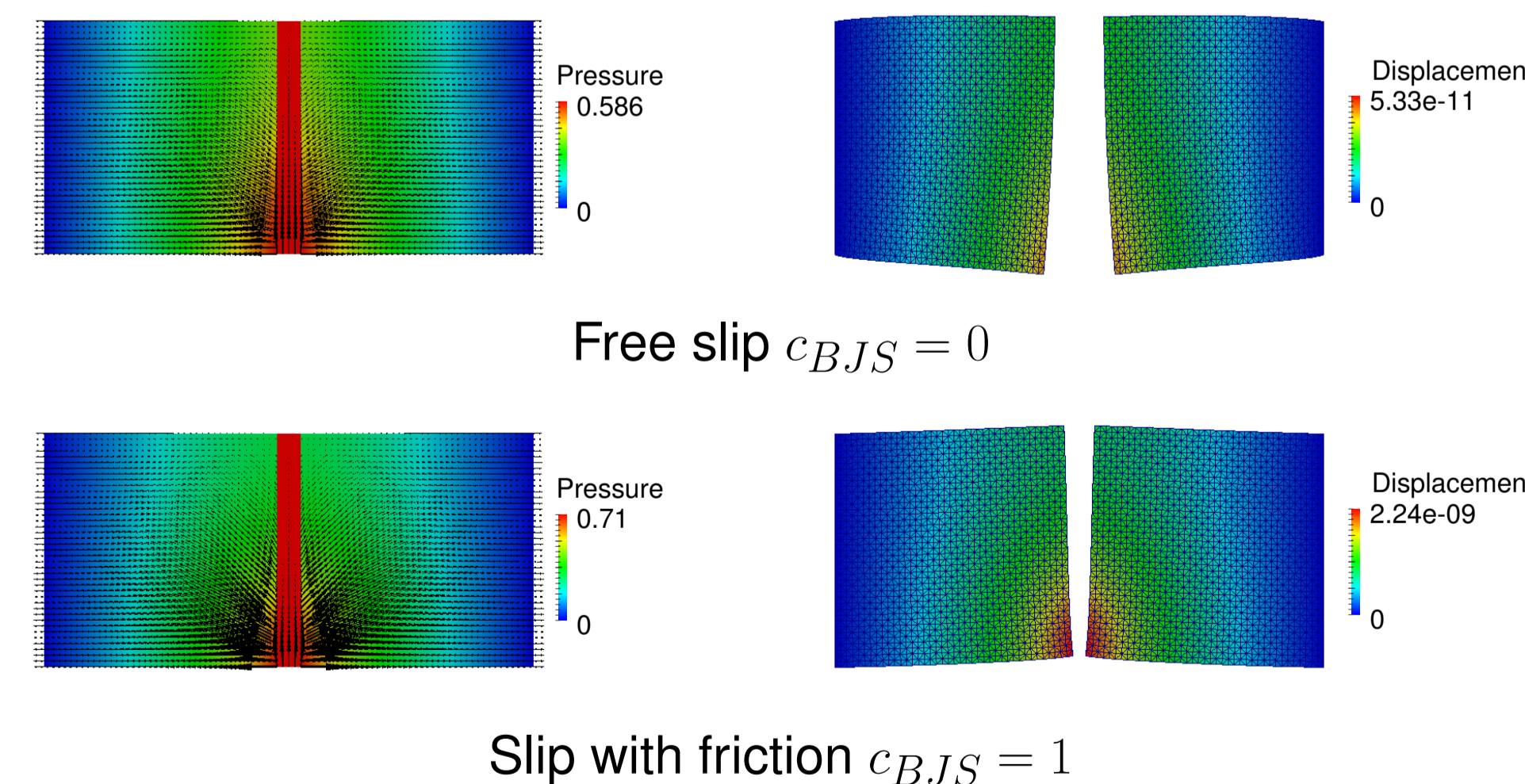
h	$\ \mathbf{u}_f - \mathbf{u}_{f,h}\ _{L^2(H^1)}$	rate	$\ \mathbf{u}_f - \mathbf{u}_{f,h}\ _{L^\infty(L^2)}$	rate
1/20	1.33e+00	0.00	9.58e-03	0.00
1/40	5.11e-01	1.38	1.87e-03	2.36
1/80	2.31e-01	1.15	3.88e-04	2.27
1/160	9.24e-02	1.32	7.07e-05	2.46

h	$\ \mathbf{u}_p - \mathbf{u}_{p,h}\ _{L^2(L^2)}$	rate	$\ p_p - p_{p,h}\ _{L^\infty(L^2)}$	rate
1/20	5.46E-02	—	4.37E-02	—
1/40	3.26E-02	0.74	2.04E-02	1.10
1/80	1.63E-02	1.00	8.74E-03	1.22
1/160	8.26E-03	0.98	2.91E-03	1.59

h	$\ \boldsymbol{\eta} - \boldsymbol{\eta}_h\ _{L^\infty(H_1)}$	rate
1/20	1.07E-01	—
1/40	5.95E-02	0.85
1/80	2.92E-02	1.03
1/160	1.05E-02	1.48

Effect of BJS condition

Figure 5. Effect of BJS condition



Continuity of flux

Table 2. Jump in fluxes across the interface, $\mathcal{R}_{\Gamma_{fp}} = \int_{\Gamma_{fp}} (\mathbf{u}_f \cdot \mathbf{n}_f + (\frac{\partial \boldsymbol{\eta}_p}{\partial t} + \mathbf{u}_p) \cdot \mathbf{n}_p)$

h	Lagrange multiplier		Nitsche	
	\mathcal{R}_{Γ_1}	\mathcal{R}_{Γ_2}	\mathcal{R}_{Γ_1}	\mathcal{R}_{Γ_2}
1/20	4.44E-12	3.86E-12	2.75E-01	2.75E-01
1/40	1.97E-12	1.97E-12	4.87E-03	4.87E-03
1/80	4.23E-13	4.24E-13	1.54E-03	1.54E-03
1/160	1.07E-13	1.06E-13	3.85E-04	3.85E-04

4. Applications to reservoir simulation

Injection-production example

Figure 7. Physical grid

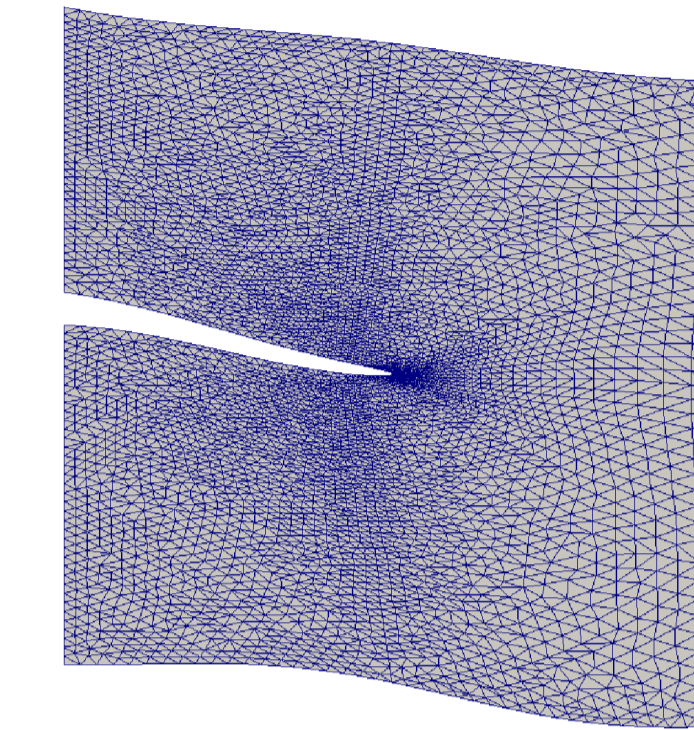
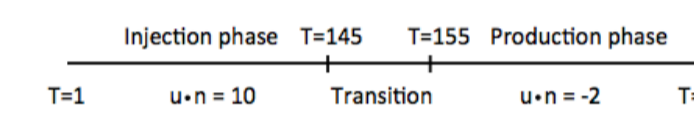


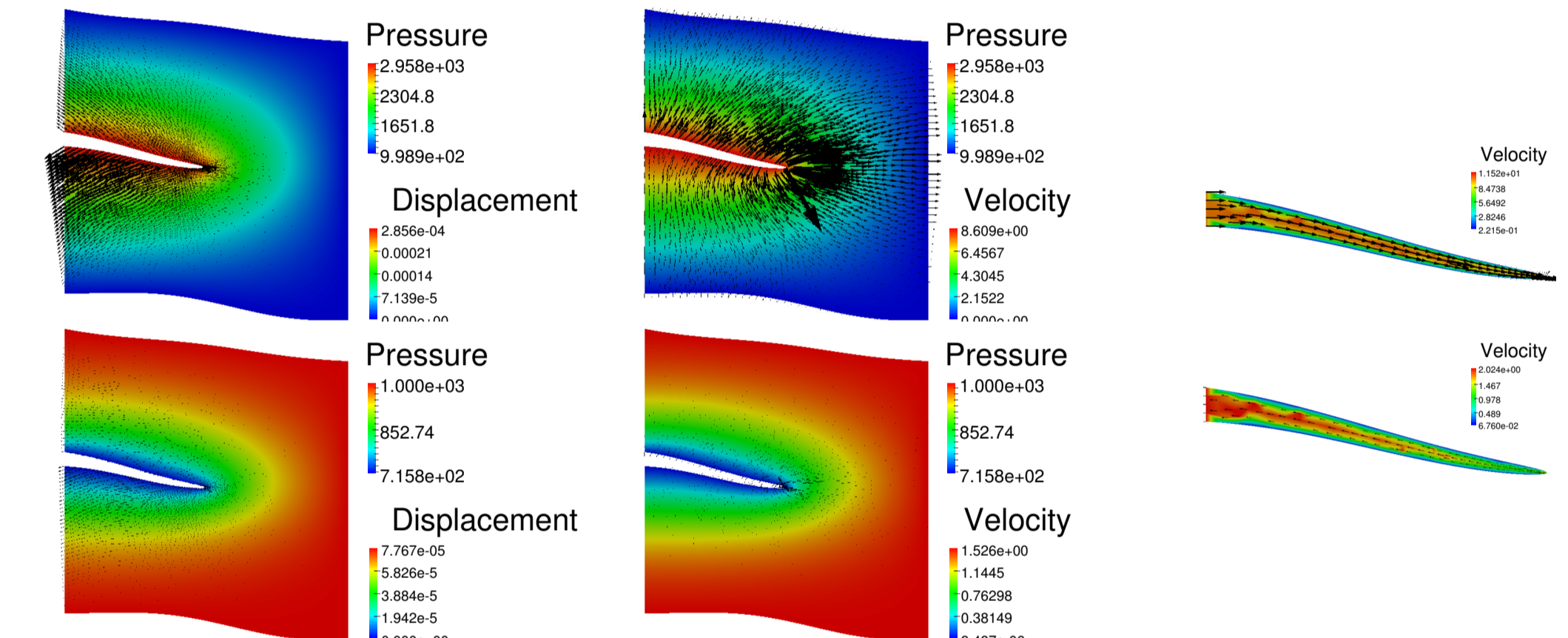
Figure 8. Phases



Parameter	Units	Value
Young's modulus	(KPa)	10^7
Fluid density	(kg/m ³)	897.0
Dynamic viscosity	(KPa s)	10^{-6}
Lame coefficient	(KPa)	$5/12 \cdot 10^7$
Lame coefficient	(KPa)	$5/18 \cdot 10^7$
Hydraulic conductivity	(m ² /KPa s)	$(200, 50) \cdot 10^{-6}$
Mass storativity	(KPa ⁻¹)	6.89×10^{-2}
Biot-Willis constant		1.0
BJS coefficient		1.0
Total time	(s)	300

$$\begin{aligned} \mathbf{u}_f \cdot \mathbf{n} &= 10, \mathbf{u}_f \cdot \boldsymbol{\tau} = 0 \text{ on } \Gamma_{inflow} \\ \mathbf{u}_p \cdot \mathbf{n} &= 0, \text{ on } \Gamma_{left} \\ p_p &= 1000, \text{ on } \Gamma_{top} \cup \Gamma_{right} \cup \Gamma_{bottom} \\ \boldsymbol{\eta} &= 0, \text{ on } \Gamma_{top} \cup \Gamma_{right} \cup \Gamma_{bottom} \end{aligned}$$

Figure 9. Last step of injection (top) and production (bottom) phases



Heterogeneous permeability example

Young's modulus: $E = E_0(1 - \frac{\phi}{0.5})^{2.1}$

Figure 10. Permeability, porosity and Young's modulus, SPE data.

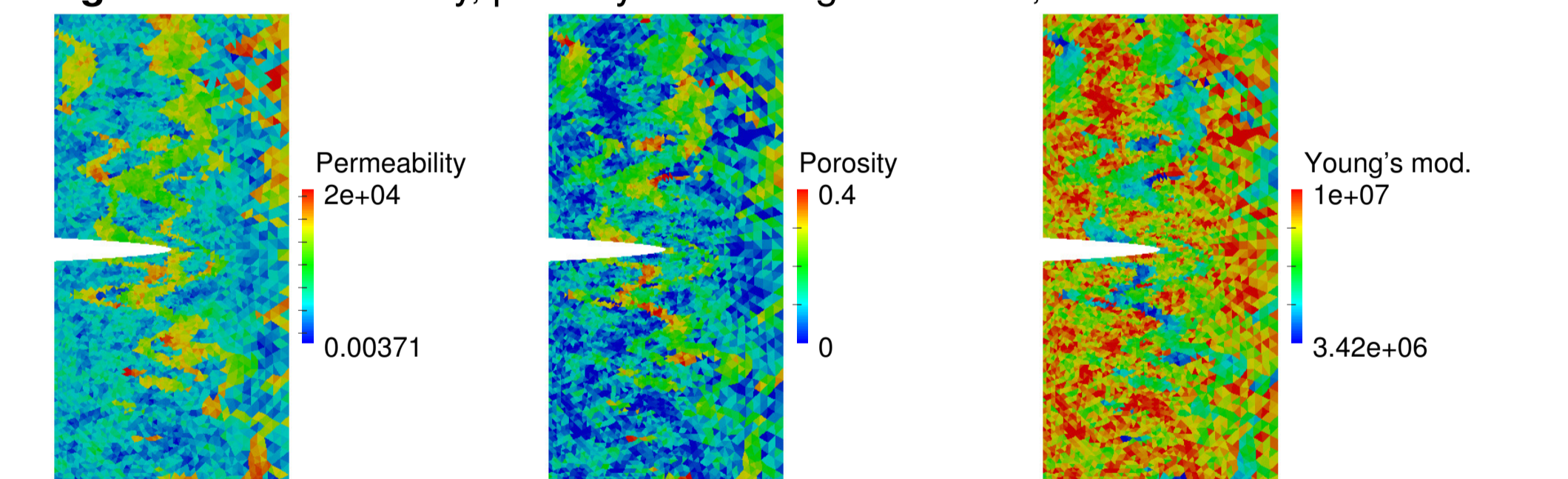
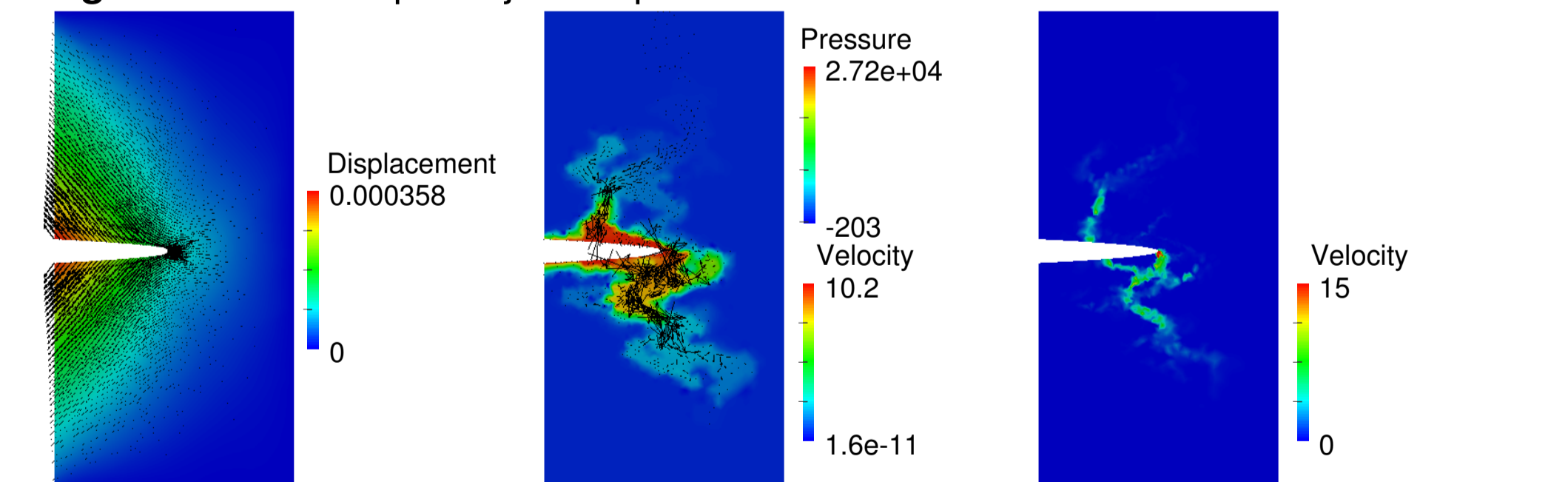


Figure 11. Last step of injection phase



5. References

- [1] I. Ambartsumyan, E. Khattatov, I. Yotov and P. Zunino. A Lagrange multiplier method for flow in fractured poroelastic media. Preprint.
- [2] M. Bukac, I. Yotov, R. Zakerzadeh and P. Zunino. Partitioning strategies for the interaction of a fluid with a poroelastic. Comput. Methods Appl. Mech. Engrg. 292 (2015) 138170.